Contents lists available at ScienceDirect

# Ultrasound in Medicine & Biology

journal homepage: www.elsevier.com/locate/ultrasmedbio

Original Contribution

# Effects of Blood Pressure on Brain Tissue Pulsation Amplitude in a Phantom Model

Jennifer K. Nicholls [a,b], Poppy Turner [a,c], Andrea Lecchini-Visintini [a,d], Jonathan Ince [a], Georgina de Vries [b], Laurie Cappellugola [a], Mitsuhiro Oura [e], Kelechi U. Ebirim [c], Edward Pallett [b], Kumar V. Ramnarine [b,g], Emma M.L. Chung [a,b,f,h,∗]

[a] Cerebral Haemodynamics in Ageing and Stroke Medicine (CHiASM) Research Group, Department of Cardiovascular Sciences, University of Leicester, Leicester, UK
[b] Department of Medical Physics, University Hospitals of Leicester NHS Trust, Leicester, UK
[c] School of Engineering, University of Leicester, Leicester, UK
[d] School of Electronics and Computer Science, University of Southampton, Southampton, UK
[e] Nihon Kohden Corporation, Tokorozawa-shi, Saitama, Japan
[f] NIHR Leicester Biomedical Research Centre, University of Leicester, Leicester, UK
[g] Medical Physics Department, Guy's and St Thomas' NHS Foundation Trust, London, UK
[h] Faculty of Life Sciences and Medicine, King's College London, London, UK

Objective: The precise mechanism and determinants of brain tissue pulsations (BTPs) are poorly understood, and the impact of blood pressure (BP) on BTPs is relatively unexplored. This study aimed to explore the relationship between BP parameters (mean arterial pressure [MAP] and pulse pressure [PP]) and BTP amplitude, using a transcranial tissue Doppler prototype.
Methods: A phantom brain model generating arterial-induced BTPs was developed to observe BP changes in the absence of confounding variables and cerebral autoregulation feedback processes. A regression model was developed to investigate the relationship between bulk BTP amplitude and BP. The separate effects of PP and MAP were evaluated and quantified.
Results: The regression model ($R^2 = 0.978$) revealed that bulk BTP amplitude measured from 27 gates significantly increased with PP but not with MAP. Every 1 mm Hg increase in PP resulted in a bulk BTP amplitude increase of 0.29 μm.
Conclusion: Increments in BP were significantly associated with increments in bulk BTP amplitude. Further work should aim to confirm the relationship between BP and BTPs in the presence of cerebral autoregulation and explore further physiological factors having an impact on BTP measurements, such as cerebral blood flow volume, tissue distensibility and intracranial pressure.

## Introduction

Previous cross-sectional healthy volunteer and physiological measurement studies have investigated factors influencing brain tissue pulsatility, demonstrating that pulse pressure (PP) is a major determinant of brain tissue pulsation (BTP) amplitude [1]. However, the exact nature of this relationship, and whether brain tissue pulsations are also influenced by mean arterial pressure (MAP), has yet to be determined.

It is widely accepted that the brain moves with every cardiac cycle [2,3]. However, the precise mechanisms and determinants of BTPs have yet to be fully understood. Based on previous findings [1,2,4] and reviews of existing magnetic resonance imaging (MRI) [5] and ultrasound literature [6], BTPs are thought to arise primarily as a direct result of the rapid filling of arterial brain volume in systole, followed by relaxation through venous drainage in diastole (Fig. 1). As the brain's compartments are almost completely enclosed in the skull and largely incompressible, this sudden increase in arterial blood volume also leads to an increase in pressure within the intracranial compartments (blood, tissue and cerebrospinal fluid [CSF]), in accordance with the Monro−Kellie doctrine [7]. Brain structures with differing physical properties may move differently in response to this temporary increase in intracranial pressure (ICP), depending on their local environment; for example, in brain regions adjacent to the foramen magnum, CSF and tissue may move toward or through the opening, resulting in larger tissue displacements in and around these regions.

This picture is broadly consistent with MRI studies, which confirm that tissue motion over the cardiac cycle is most pronounced at the base of the brain, around the region of the foramen magnum, where both CSF and tissue are displaced downward towards the spinal canal in systole [3]. During diastole, as arterial volume returns to its original value

---

∗ Corresponding author. Faculty of Life Sciences and Medicine, King's College London, London WC2R 2LS, UK.
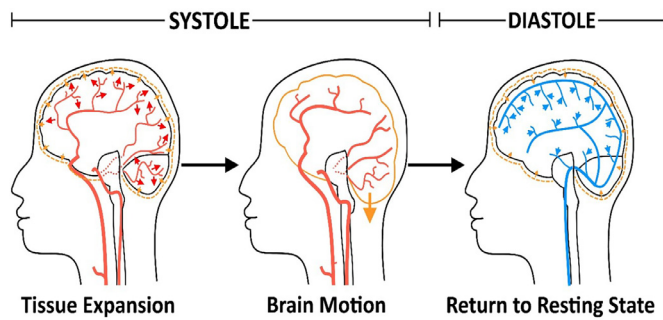E-mail address: emma.chung@kcl.ac.uk (E.M.L. Chung).

**Figure 1.** Hypothesis concerning the origins of artery-induced brain tissue pulsations. The *small red arrows* indicate major artery expansion in systole, and the *small orange arrows* indicate the direction of tissue motion. The *large orange arrow* demonstrates the direction of global brain motion in systole. The *small blue arrows* indicate the direction of tissue motion during diastole. During diastole, venous outflow exceeds arterial inflow and the brain returns to begin the cycle again.

through venous drainage, the brain compartments return to their original shape and volume. Over successive heart beats, this generates periodic motion synchronised with the cardiac cycle [7]. Currently, the relative contributions to brain tissue motion of (i) local major artery pulsations and (ii) ICP-mediated redistribution of brain compartments are unclear. Other factors contributing to brain tissue motion might include contractile effects (reductions in the length of arteries as they expand) and cardioballistic effects (tissue "recoil") in response to cardiac ejection.

In previous work, pulsation of the artery walls has been shown to propagate into adjacent tissue, generating localised pulsatile tissue motion superimposed on global motion [1]. A previous cross-sectional healthy volunteer study by Turner et al. [1] found that MAP was not a significant predictor of bulk BTP amplitude at a population level. However, a positive association was noted between baseline bulk BTP amplitude (measured at the forehead) and baseline PP.

A clear understanding of the relationship between blood pressure (BP) and BTPs is required to enable further exploration of the clinical applications of BTP measurements. In this study, we developed a simplified ultrasound brain phantom generating artery-induced BTPs under controlled conditions. This setup allowed us to quantify the relationship between BP parameters (MAP and PP) and bulk BTP amplitude, measured using transcranial tissue Doppler (TCTD), in the absence of confounding variables and cerebral autoregulation feedback processes.

## Methods

Our phantom model comprised a 3-D PolyJet VeroWhite skull, reported to have similar ultrasound attenuation properties as the human

skull [8]. The skull *.stl mesh was sourced from Thingiverse.com and imported to MeshLab (Institute of Information Science and Technologies-Italian National Research Council, University of Pisa, Pisa, Italy), where it was checked for integrity and adapted to house a vascular replica of the major cerebral arteries.

The "skull" was 3-D-printed using a Stratasys Objet 330 printer (Eden Prairie, MN, USA, and Rehovot, Israel) and an anatomically accurate silicone replica of the major cerebral arteries (Elastrat, Geneva, Switzerland) was positioned within the skull (Fig. 2). The silicone cerebral artery replica included four inlets (bilateral carotid and vertebral arteries) that entered the skull through the foramen magnum and three outlets that left the phantom through three holes added to the model cranium. One outlet combined both anterior cerebral arteries (ACAs); the other two outlets combined the middle cerebral artery (MCA) and posterior cerebral artery (PCA) outlets for the left and right hemispheres. Each outlet was made from Cole-Parmer C-flex tubing (Cole-Parmer Instrument Company Ltd, Cambridgeshire, UK) with an external diameter of 4 mm and an internal diameter of 2.29 mm. The arterial replica was carefully positioned within the skull and the top plate of the skull made water tight using silicone sealant.

The model arteries were then surrounded by a soft polyvinyl-alcohol cryogel (c-PVA) tissue-mimicking material (TMM). Approximately 3 L of a validated c-PVA ultrasound TMM with properties mimicking soft brain tissue was used to fill the phantom while inverted. The TMM composition was 79.4% water, 9.6% glycerol, 9.6% polyvinyl alcohol (PVA), 0.5% of 3 μm calcinated aluminium oxide, 0.4% of 0.3 μm ultra-fine aluminium oxide, 0.3% of silicon carbide, and 0.003% of benzalkonium chloride. The recipe and manufacture of the TMM was based on previous reports [9−11]. The mixture was placed in a water bath at an initial temperature of 45°C and a final temperature of 97°C for 2.5 h, with continuous stirring. The mixture was then cooled and poured into the up-turned phantom skull through the foramen magnum, leaving a small gap to allow for expansion during the freezing process. The number of freeze−thaw cycles aimed to mimic the acoustic and elastic properties of human brain tissue: speed of sound = 1550 m/s [12], density = 1.03 g/cm$^3$ [12] and Young's Modulus = 14.9 kPa [13].

Approximately 1.2 L of a validated blood-mimicking fluid (BMF) solution circulated through the silicone replica arteries under physiological flow conditions generated by a programmable pump, created by the University Hospitals of Leicester Clinical Engineering Scientific Services team. The BMF solution comprised 83.9% water, 10.1% glycerol, 3.4% dextran, 1.8% Orgasol particles, and 0.9% surfactant [14]. The resulting BMF viscosity is a good match to blood at ∼4 mPas [14]. The components were mixed for 1 h using a magnetic stirrer and then sieved using a 53-μm sieve before use.

Physiological conditions were implemented and validated within the phantom prior to data collection. Physiological pressures were achieved by appropriately selecting peripheral resistance tubing attached to the
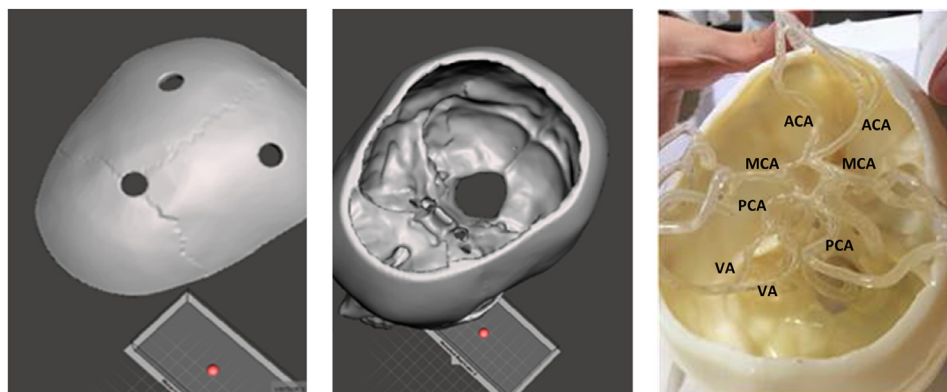


**Figure 2.** (a, b) STL files for the 3-D-printed phantom brain model. (c) The 3-D-printed skull and labelled silicone artery replica positioned within the phantom, containing the middle cerebral arteries (ACA), middle cerebral arteries (MCA), posterior cerebral arteries (PCA) and vertebral arteries (VA).
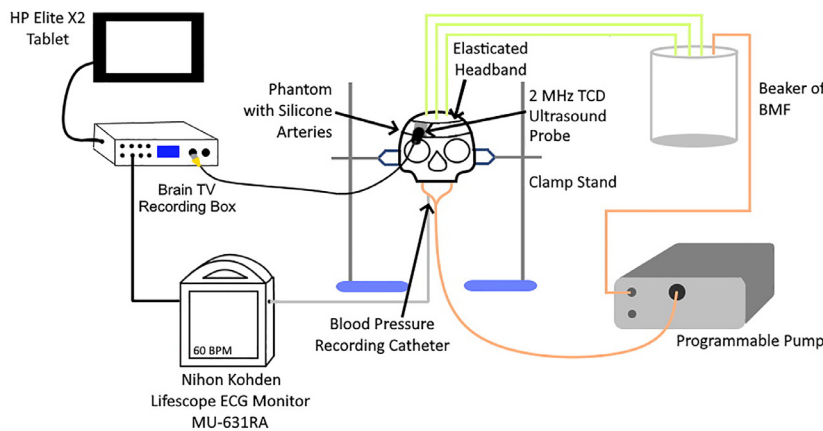
**Figure 3.** Schematic of the phantom setup connected to the Brain Tissue Velocimetry (TV) measurement system.

vessel outlets and inlets according to an electrical analogue model approach [15]. This also ensured that ∼75% of the total blood flow (BMF flow) passed through the anterior circulation and ∼25% passed through the posterior circulation. Pump settings were adjusted to achieve a physiological BP trace, flow rate and heart rate (HR) of 60 bpm. Flow rates were verified before each experiment through timed collection of fluid, which was repeated three times and averaged.

A pressure transducer was introduced to the phantom circulation through the "right external carotid artery" of the phantom to obtain continuous BP measurements, using an electrocardiogram (ECG) Lifescope monitor MU-631RA (Nihon Kohden, Tokyo, Japan). TCTD measurements were recorded from the right forehead of the phantom using a data acquisition prototype (Brain Tissue Velocimetry [Brain TV]; Nihon Kohden), equipped with a 2 MHz single-element transcranial Doppler (TCD) probe (Spencer Technologies, MA, USA), as shown in Figure 3.

To validate physiological conditions within the phantom, a healthy adult comparator provided written informed consent, following a protocol approved by the University of Leicester Medicine and Biological Sciences Research Ethics Committee, and in accordance with the Declaration of Helsinki (2013).

Two experiments were carried out on the phantom to determine the effect of MAP and PP on BTPs. PP is defined as the systolic blood pressure (SBP) minus the diastolic blood pressure (DBP) ($SBP − DBP$), whilst MAP is defined as $DBP + \frac{1}{3}(SBP − DBP)$. MAP was raised by increasing the pressure difference across the phantom through raising the height of the BMF reservoir whilst maintaining constant flow. The BMF reservoir was raised by 20 cm every 20 s over 3 min, resulting in eight different MAP values within one continuous recording. The flow rate used for the MAP experiment was 650 mL/min, replicating the flow of blood into the brain [16]. In our second experiment, PP was altered by increasing the amplitude of the output flow waveform generated by the programmable pump. This increased PP from ∼12 to ∼100 mm Hg over a series of seven recordings. A 10-s recording for each amplitude setting was obtained.

The flow pump occasionally generated vibrations when set to higher amplitudes, causing motion artefacts to be observed. This was minimised by securing the phantom using a clamp and placing the pump on a different surface to the phantom and Brain TV system. Cables were secured to avoid motion artefacts.

*Data analysis*

Brain tissue pulsation and BP recordings from the phantom were gathered and analysed using a graphical user interface (GUI) developed in-house using MATLAB (R2021a). In-phase and quadrature-phase (IQ) data from each TCTD recording were down-sampled to 0.5 kHz to reduce file sizes, giving a temporal resolution of 2 ms. Tissue velocity at each depth was estimated using the S-Dopp velocity estimator [17]. This estimator combines Doppler signals from different subsample volumes. In our implementation, three subsample volumes were combined over one pulse length. Tissue velocity estimates were integrated over time to produce a BTP signal representing real-time displacement at each tissue depth.

Brain tissue pulsations measurements were obtained from 33 sample depths within the phantom brain, ranging from 22 to 86 mm below the probe's surface. Each depth provides a measurement of tissue velocity in the direction of the ultrasound beam from a cylindrical ∼3-mm high × 5-mm diameter volume of brain tissue. Adjacent depths were separated by 2 mm, resulting in a series of overlapping sample volumes.

As this phantom experiment was performed under controlled conditions, all data were artefact-free; however, depths associated with poor signal-to-noise were discarded. A bulk BTP signal was calculated for each recording by calculating the average BTP across all depths from which a good BTP signal was obtained, representing collective displacement of the phantom 'brain' over the cardiac cycle.

*Statistical analysis*

Beat-to-beat estimates for PP, MAP and bulk BTP amplitude were obtained using MATLAB (R2021a). For both phantom experiments, these beat-to-beat values for each variable were averaged over a consistent 8-s interval chosen in the middle of each BP experiment, to obtain representative values for each.

A regression model was developed to investigate the relationship between bulk BTP amplitude and BP. Eight 8-s intervals from the MAP experiment and six 8-s intervals from the PP experiment were used in the model, resulting in 14 bulk BTP amplitude values. Regression coefficients were obtained with STATA version 17.0 (StataCorp LLC) using the regress command with default options. The regression model was expressed in terms of MAP and PP and alternatively in terms of SBP and DBP following a suitable change of coordinates obtained using the lincom command.

The statistical significance level was set at the standard value $p = 0.05$.

**Results**

Brain tissue pulsations measured from 27 depths (up to a maximum depth of 74 mm) were adequately visualised during the MAP experiment and 30 depths (up to a maximum depth of 86 mm) during the PP experiment. This slight difference in penetration depth is likely to be due to a slight difference in probe positioning between experiments, with the probe placed on a thicker portion of the phantom skull during the MAP experiment. For consistency, the bulk BTP signal was calculated using 27 depths for both experiments.

Bulk BTP amplitude in the phantom and a healthy subject were qualitatively compared for validation purposes. Bulk BTP amplitude was clearly seen to increase with depth into the phantom brain, which is consistent with observations in healthy subjects, as shown in Figure 4. A
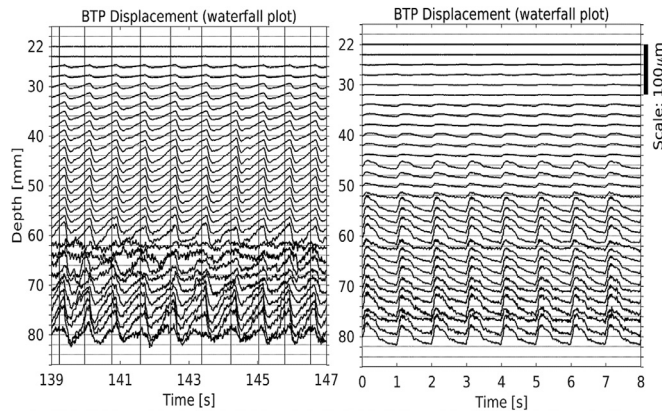
**Figure 4.** Waterfall plots for a 29-y-old male healthy volunteer with a pulse pressure (PP) of 53.8 mm Hg (left) and the phantom, operating with a physiological PP of 58.3 mm Hg (right). Both the general waveform shape and amplitude are similar between the phantom and healthy volunteer. BTP, brain tissue pulsation.

clear peak and trough with each cardiac cycle was visible and the magnitude of pulsations were similar to those observed in the healthy subject.

MAP was successfully increased in the phantom, from 86 to 228 mm Hg, by altering the height of the BMF reservoir. This resulted in an increase in MAP of +142 mm Hg. PP slightly increased during this protocol by ΔPP = +6 mm Hg, from 113 to 119 mm Hg. These increases in BP corresponded to a bulk BTP amplitude (measured from 27 depths) change ΔBTP = +0.3 μm, from 18.3 to 18.6 μm, which is below measurement accuracy. Figure 5 demonstrates the changes in BP and bulk BTP amplitude in the phantom over time.

Using the second experiment protocol, PP in the phantom increased from 12 to 101 mm Hg, accompanied by an increase in MAP from 38 to 79 mm Hg. These changes in BP resulted in a significant increase in bulk BTP amplitude (measured from 27 depths) of +24.5 μm, from the lowest PP value of 3.7 μm to the highest PP value of 28.2 μm. Figure 6 shows the changes in BP and bulk BTP amplitude over time.

This preliminary analysis indicated that changing MAP had little effect on bulk BTP amplitude whilst changing PP had a significant effect. A regression model was estimated to confirm these findings. Values of MAP, PP, SBP, DBP and bulk BTP amplitude measured from 27 depths, obtained from both experiments, were aggregated in order to perform
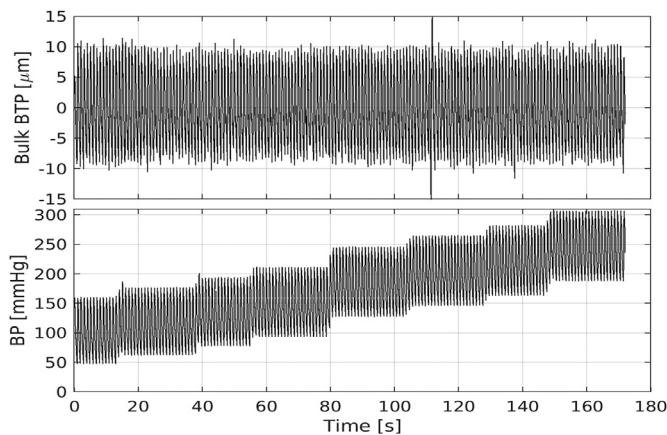


**Figure 5.** Blood pressure (BP) and bulk brain tissue pulsation (BTP) changes in response to increasing mean arterial pressure (MAP) in the phantom, induced by increasing the height of the blood-mimicking fluid reservoir, over a recording period of 172 s. In this experiment, an increase in systolic blood pressure (SBP) is accompanied by an increase in diastolic blood pressure (DBP) with pulse pressure remaining approximately constant. SBP increased from a starting value of 161 to 307 mm Hg and DBP increased from 48 to 188 mm Hg.
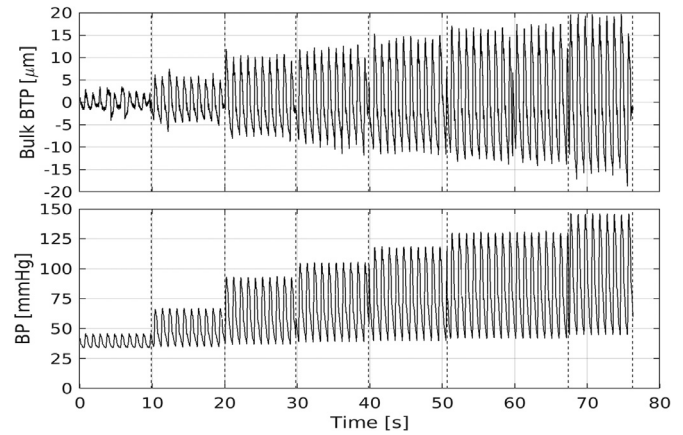


**Figure 6.** Responses of Blood Pressure (BP) and bulk brain tissue pulsation (BTP) in response to increasing pulse pressure (PP) in the phantom induced by altering the amplitude of the waveform output of the programmable pump, over a recording period of 77 s. The *dashed vertical lines* indicate that the experiment was paused so that pump settings could be changed between recordings. The increase in PP was largely achieved through increasing systolic blood pressure from 46 to 146 mm Hg; however, diastolic blood pressure also increased slightly during this experiment from 34 to 45 mm Hg.

regression analysis, since the experimental data within each experiment were collinear. Initial analysis showed a small constant bias difference between the two experiments, which was well captured by including a categorical variable. The regression model, by means of a change of coordinates, was also used to confirm the relationship with SBP and DBP values.

The expression of the regression model in PP/MAP coordinates or alternatively in SBP/DBP coordinates is given as

$$BTP = a\,SBP + b\,DBP + \delta\,EXP + const$$

$$= \alpha\,PP + \beta\,MAP + \delta\,EXP + const$$

where a and b are the slope coefficients in the SBP/DBP coordinates, $\alpha$ and $\beta$ are slope coefficients in the PP/MAP coordinates, EXP (= 0/1 in the MAP/PP experiment) is a categorical variable and const is the intercept. The coefficients $\delta$ and const have the same values in both coordinates. The results of the model are given in Table 1.

The regression model achieved a very good fit ($R^2 = 0.978$), showing that the relation between BP variables and bulk BTP amplitude is almost linear for the experimental conditions considered in this study. In the PP/MAP coordinates, the model confirmed a significant relationship between PP and bulk BTP amplitude and that the effect of MAP was not significant. In the SBP/DBP coordinates, no significant difference in the absolute values of the effects of SBP and DBP was found, thus

**Table 1**

Model coefficients, 95% CIs and *p* values for each of the variables in the regression model

| Coefficient | Variable | Estimate (95% CI) | *p* Value |
|---|---|---|---|
| Slope coefficients in SBP/ DBP coordinates | SBP (a) | 0.284 (0.255−0.312) | $<10^{-3}$ |
| | DBP (b) | −0.291 (−0.326 to −0.256) | $<10^{-3}$ |
| Slope coefficients in PP/ MAP coordinates | PP ($\alpha$) | 0.286 (0.256−0.316) | $<10^{-3}$ |
| | MAP ($\beta$) | −0.007 (−0.024 to 0.009) | 0.347 |
| Coefficients with same values in both coordinates | EXP ($\delta$) | 14.587 (12.408−16.765) | $<10^{-3}$ |
| | Intercept (const) | −13.941 (−17.625 to −10.257) | $<10^{-3}$ |

DBP, diastolic blood pressure; EXP, experiment categorical variable; MAP, mean arterial pressure; PP, pulse pressure; SBP, the systolic blood pressure.

confirming that their effects are symmetric (increasing SBP has the same effect as decreasing DBP).

## Discussion

This study explored the relationship between arterial BP (MAP and PP) and BTP amplitude in a passive phantom brain model, comprising a replica of the major arteries, soft tissue and a skull model. Our results suggest that cerebral arterial PP, but not MAP, has a significant impact on BTP amplitude.

Both PP and MAP were significantly altered in the phantom under controlled conditions. Under constant flow conditions, bulk BTP amplitude was found to mirror changes in PP. Alterations in MAP had no discernible impact. The first phantom experiment resulted in a large increase in MAP, while PP and bulk BTP amplitude remained relatively constant, suggesting that MAP alone has no impact on bulk BTP amplitude. The second phantom experiment resulted in a large increase in PP, accompanied by a much smaller increase in MAP. An increase in PP of 89 mm Hg resulted in a significant increase in bulk BTP amplitude of $\Delta BTP = +24.5$ μm, indicating that bulk BTP amplitude was influenced greatly by PP. A regression model confirmed the significant association between PP increases and bulk BTP amplitude and that the effect of MAP is not significant.

Our results also agree with Alharbi et al. [2], who noted an increase in both arterial PP and bulk BTP amplitude following a hyperventilation manoeuvre in 30 healthy volunteers. In that study [2], MAP decreased in response to hypocapnia, but it was difficult to determine whether the observed BTP changes were the result of the increase in PP, decrease in MAP or other physiological factors. This study suggests that the observed increase in bulk BTP amplitude during hypocapnia is likely to be explained by the increase in PP that accompanied this manoeuvre [2].

Turner et al. [1] previously investigated variability in bulk BTP amplitude measurements from a cross-section of a healthy population to explore whether age, sex, PP, MAP and HR impacted bulk BTP amplitude. Healthy brain tissue motion was studied to understand which variables affected tissue motion at the forehead and temporal positions [1]. A multivariate linear regression analysis identified PP as a significant factor explaining bulk BTP amplitude variability at a population level. A 1% increase in brachial artery PP between subjects resulted in a 0.8% increase in baseline bulk BTP amplitude measured through the forehead (calculated by averaging BTP signals across 30 depths; $p < 0.001$) [1]. No significant association of BTP amplitude with MAP was noted [1]. The results of our study confirm these findings; the phantom was used to alter BP in the absence of confounding variables and increases in PP and bulk BTP amplitude were found to be significantly correlated.

Our phantom model approximated the dimensions of a human head and coupling of tissue pulsations with physiologically realistic pulsatile blood flow, providing a useful tool for exploring factors affecting BTPs under controlled conditions. The flow of BMF accurately replicated cerebral blood flow (CBF) within the major arteries, with a waveform chosen to mimic the pulsatile blood flow generated by the heart.

Our findings suggest that bulk BTP amplitude is related to major artery PP, but other factors such as the impact of CBF, ICP or tissue stiffness have yet to be explored [4]. A greater understanding of the relationship between BP and BTPs is important for clinical translation; BTP amplitude varies widely between participants due to variations in PP, making it important to be able to adjust for PP when interpreting BTP features. It might also be possible to control excessive BTPs through the use of BP lowering medication.

Previous literature has suggested excessive brain motion is correlated with brain atrophy [18], cerebrovascular disease [18] and cognitive decline in elderly patients, following damage to the cerebral microcirculation [19]. Targeting excessive pulsatility and large variations in CBF reactivity, such as modulating vascular tone of the MCA [20], may reduce the risk of cerebrovascular disease in the elderly. Alongside

TCTD, other imaging methods have been trialled to characterise BTPs in health and disease, such as tissue pulsatility imaging (TPI) [18,20−22] and phase contrast MRI [19]. TPI has been suggested to detect an increase in brain motion and changes in brain vascular function in mid-life depression, placing these patients at a higher risk of cerebrovascular disease [18]. Monitoring BTPs may also be useful in elderly patients with orthostatic hypotension (OH); Biogeau et al. [23] previously identified a significant decrease in BTPs in patients with OH after 1 min of standing. Further work should focus on exploring the clinical applications of BTP measurements and the relationship between BTPs and other factors.

### Limitations and future work

Phantom studies are associated with numerous limitations, and our simplified "passive" model of brain tissue motion is no exception. The model features a major internal circulation with no perforating vessels and the TMM used is homogenous and non-porous, so is not perfused in the same way as real tissue. The wall of the arterial replica was thicker (~1 mm) and less elastic than those of real arteries, likely leading to lower artery-induced BTP amplitudes than in humans. Although the brain tissue was "tethered" to the arterial circulation and placed within a skull mimic, it was not surrounded by CSF, so our phantom was not capable of replicating more complex coupling among cerebral haemodynamics, tissue and CSF. Representing a passive system, the phantom was not capable of naturally reproducing cerebral autoregulatory responses. Future studies should explore the impact of cerebral autoregulation on CBF, arterial resistance and BP through additional manipulation of the model parameters and include CSF and more realistic anatomy.

Deeper gates affected by noise were not analysed, so only tissue motion was quantified. Depths were explored based on visual inspection; this could be automated based on ultrasound echo intensity analysis in the future.

The regression model identified a bias between experiments, likely due to the two experiments being performed on different days. We cannot guarantee that the setup remained exactly the same, including the positioning of the probe onto the phantom skull. However, the probe would have been adjusted until clear pulsations were observed and the magnitude of pulsations in both experiments are similar.

## Conclusion

This study found that bulk BTP amplitude mirrors changes in arterial PP and that isolated changes in MAP have little impact. The results of this study contribute to our growing understanding of the origins and factors affecting BTPs. Future work should aim to precisely model the relationship between BTPs and cerebrovascular physiology, including CBF, ICP, HR and changes in arterial and brain tissue stiffness.

## Conflict of interest

The authors declare no competing interests.

## Data availability statement

Our real-time physiological measurement data are unsuitable to post online because of large file sizes and the requirements of bespoke software for data visualisation. Summary data are available through requesting access from the corresponding author.

## References

[1] Turner P, Banahan C, Alharbi M, Ince J, Venturini S, Berger S, et al. Brain tissue pulsation in healthy volunteers. Ultrasound Med Biol 2020;46:3268–78.

[2] Alharbi M, Turner P, Ince J, Oura M, Ebirim KU, Almudayni A, et al. The effects of hypocapnia on brain tissue pulsations. Brain Sci 2020;10:614.

[3] Wagshul ME, Eide PK, Madsen JR. The pulsating brain: a review of experimental and clinical studies of intracranial pulsatility. Fluids Barriers CNS 2011;8:5.

[4] Ince J, Banahan C, Venturini S, Alharbi M, Turner P, Oura M, et al. Acute ischemic stroke diagnosis using brain tissue pulsations. J Neurol Sci 2020;419:117164.

[5] Almudayni A, Alharbi M, Chowdhury A, Ince J, Alablani F, Minhas JS, et al. Magnetic resonance imaging of the pulsing brain: a systematic review. MAGMA 2022;36:3–14.

[6] Ince J, Alharbi M, Minhas JS, Chung EML. Ultrasound measurement of brain tissue movement in humans: a systematic review. Ultrasound 2019;28:70–81.

[7] Kim DJ, Czosnyka Z, Kasprowicz M, Smieleweski P, Baledent O, Guerguerian AM, et al. Continuous monitoring of the Monro−Kellie doctrine: Is it possible? J Neurotrauma 2011;29:1354–63.

[8] Robertson J, Martin E, Cox B, Treeby BE. Sensitivity of simulated transcranial ultrasound fields to acoustic medium property maps. Phys Med Biol 2017;62:2559–80.

[9] Malone AJ, Cournane S, Naydenova IG, Fagan AJ, Browne JE. Polyvinyl alcohol cryogel based vessel mimicking material for modelling the progression of atherosclerosis. Phys Med 2020;69:1–8.

[10] Cournane S, Cannon L, Browne JE, Fagan AJ. Assessment of the accuracy of an ultrasound elastography liver scanning system using a PVA−cryogel phantom with optimal acoustic and mechanical properties. Phys Med Biol 2010;55:5965–83.

[11] Al-Mutairi FF, Chung EM, Moran CM, Ramnarine KV. A novel elastography phantom prototype for assessment of ultrasound elastography imaging performance. Ultrasound Med Biol 2021;47:2749–58.

[12] Azhari H. Basics of biomedical ultrasound for engineers. New York: Wiley; 2010.

[13] Chan HW, Uff C, Chakraborty A, Dorward N, Bamber JC. Clinical application of shear wave elastography for assisting brain tumor resection. Front Oncol 2021;11:619286.

[14] Ramnarine KV, Nassiri DK, Hoskins PR, Lubbers J. Validation of a new blood-mimicking fluid for use in Doppler flow test objects. Ultrasound Med Biol 1998;24:451–9.

[15] Chung EML, Hague JP, Chanrion MA, Ramnarine KV, Katsogridakis E, Evans DH. Embolus trajectory through a physical replica of the major cerebral arteries. Stroke 2010;41:647–52.

[16] Scheel P, Ruge C, Schöning M. Flow velocity and flow volume measurements in the extracranial carotid and vertebral arteries in healthy adults: reference data and the effects of age. Ultrasound Med Biol 2000;26:1261–6.

[17] Hoeks APG, Brands PJ, Arts TGJ, Reneman RS. Subsample volume processing of Doppler ultrasound signals. Ultrasound Med Biol 1994;20:953–65.

[18] Desmidt T, Brizard B, Dujardin PA, Ternifi R, Réméniéras JP, Patat F, et al. Brain tissue pulsatility is increased in midlife depression: a comparative study using ultrasound tissue pulsatility imaging. Neuropsychopharmacology 2017;42:2575–82.

[19] Wahlin A, Ambarki K, Birgander R, Malm J, Eklund A. Intracranial pulsatility is associated with regional brain volume in elderly individuals. Neurobiol Aging 2014;35:365–72.

[20] Desmidt T, Dujardin PA, Brizard B, Réméniéras JP, Gissot V, Dufour-Rainfray D, et al. Decrease in ultrasound brain tissue pulsations as a potential surrogate marker of response to antidepressant. J Psychiatr Res 2022;146:186–91.

[21] Desmidt T, Andersson F, Brizard B, Dujardin PA, Cottier JP, Patat F, et al. Ultrasound measures of brain pulsatility correlate with subcortical brain volumes in healthy young adults. Ultrasound Med Biol 2018;44:2307–13.

[22] Ternifi R, Cazals X, Desmidt T, Andersson F, Camus V, Cottier JP, et al. Ultrasound measurements of brain tissue pulsatility correlate with the volume of MRI white-matter hyperintensity. J Cereb Blood Flow Metab 2014;34:942–4.

[23] Biogeau J, Desmidt T, Dujardin PA, Ternifi R, Eudo C, Vierron E, et al. Ultrasound tissue pulsatility imaging suggests impairmant in global brain pulsatility and small vessels in elderly patients with orthostatic hypotension. J Stroke Cerebrovasc Dis 2017;26:246–51.